Possibility to synthesize $Z = 120$ superheavy nuclei with $Z > 20$ projectiles

S. H. Zhu (朱世豪) and Xiao Jun Bao (包小军)*

Department of Physics, Collaborative Innovation Center for Quantum Effects, and Key Laboratory of Low Dimensional Quantum Structures and Quantum Control of Ministry of Education, Hunan Normal University, Changsha 410081, People's Republic of China

(Received 20 April 2023; accepted 28 June 2023; published 12 July 2023)

Evaporation residue cross sections (ERCSs) for heavy-ion fusion reactions are calculated by using the dinuclear system model combined with the statistical model. The calculated results reproduce well the experimental trends of the $3n$ and $4n$ channel cross sections of $^{48}\mathrm{Ca}+{}^{238}\mathrm{U}$, $^{48}\mathrm{Ca}+{}^{244}\mathrm{Pu}$, and $^{48}\mathrm{Ca}+{}^{248}\mathrm{Cm}$. To synthesize a new element $Z = 120$, we predicted evaporation residue cross sections for four reaction systems ($^{54}\mathrm{Cr}+{}^{248}\mathrm{Cm}$, $^{58}\mathrm{Fe}+{}^{244}\mathrm{Pu}$, $^{64}\mathrm{Ni}+{}^{238}\mathrm{U}$, and $^{50}\mathrm{Ti}+{}^{249}\mathrm{Cf}$) to select the most promising projectile-target combinations. From detailed analysis of the evaporation residue cross section of synthetic superheavy nuclei, we found that the $^{54}\mathrm{Cr}+{}^{248}\mathrm{Cm}$ reaction is optimal and the maximum cross sections of the $3n$ and $4n$ channels are 17.58 and 1.09 fb. However, we also noticed that the ERCSs for the $^{54}\mathrm{Cr}+{}^{248}\mathrm{Cm}$ reaction channel predicted by our model and various other approaches are all in the range of a few femtobarns, which appears to be below the detectable limit of the currently available facilities. Thus, an increase of beam intensities, detection techniques, and efficient separation are needed to synthesize $Z = 120$ superheavy nuclei.

DOI: 10.1103/PhysRevC.108.014604

I. INTRODUCTION

In the last few decades, to explore the charge and mass limit of the nucleus [1,2], low-energy heavy-ion fusion reactions have been widely used to synthesize superheavy nuclei. Two different experimental methods [3–5] have been used to synthesize superheavy nuclei: The hot-fusion reaction performed mainly at the Joint Institute for Nuclear Research-Flerov Laboratory of Nuclear Reactions, Dubna, and the cold fusion reaction performed mainly at GSI, Darmstadt [5–7], and at Rikagaku Kenkyusho, Japan [8]. Using the cold fusion approach, the nuclei with $Z = 107$–112 have been synthesized [5–8], and the hot-fusion reaction has led to the discoveries of elements with $Z = 113$–118 [9–12]. So far, considerable progress has been made in experimental and theoretical research in the field of superheavy nuclei [13,14].

Several recent studies have suggested some projectile-target combinations may be the efficient method for the production of new superheavy nuclei ($Z = 119$ and 120). However, the actual possibilities to achieve this objective must be carefully examined. For experimentalists, it is crucial to choose the most promising projectile-target combination. Up to now, the synthesis of superheavy nuclei with $Z > 118$ has faced many experimental challenges. For example, fusion evaporation reactions using projectiles heavier than $^{48}\mathrm{Ca}$ would be required because $^{249}\mathrm{Cf}$ is the heaviest known target. To synthesize new elements beyond oganesson ($Z = 118$), heavier beams such as $^{50}\mathrm{Ti}$, $^{54}\mathrm{Cr}$, $^{58}\mathrm{Fe}$, and $^{64}\mathrm{Ni}$ have been adopted by experimentalists and theorists. Experimentally, attempts to produce $Z = 119$ and 120 have been made in the last decade in different laboratories, using various combinations of projectile and target nuclei. However, no events have been observed [15–24].

Theoretically, various theoretical models have been developed to predict the evaporation residual cross sections. However, these predicted cross sections differ by 1–5 orders of magnitude and also the excitation function peak energies differ by several MeV for a fixed projectile-target combination. Inspired by experimental data and significantly different theoretical results obtained from various theoretical models, we selected four projectile-target combinations for theoretical calculations, $^{54}\mathrm{Cr}+{}^{248}\mathrm{Cm}$ [25–28], $^{58}\mathrm{Fe}+{}^{244}\mathrm{Pu}$ [29–31], $^{64}\mathrm{Ni}+{}^{238}\mathrm{U}$ [29,31–33], and $^{50}\mathrm{Ti}+{}^{249}\mathrm{Cf}$ [25,26,28,31,34], aiming to select the optimal projectile-target combination for the synthesis of $Z = 120$.

II. THEORETICAL FRAMEWORK

In the dinuclear system (DNS) concept, the evaporation residue cross section (ERCS) is calculate as the summation over all partial waves J [35],

$$\sigma_{\mathrm{ER}}(E_{\mathrm{c.m.}}) = \sum_{J} \sigma_{\mathrm{cap}}(E_{\mathrm{c.m.}}, J) P_{\mathrm{CN}}(E_{\mathrm{c.m.}}, J) W_{\mathrm{sur}}(E_{\mathrm{c.m.}}, J), \tag{1}$$

where $E_{\mathrm{c.m.}}$ is the incident energy in the center-of-mass frame. The capture cross section σ_{cap} is calculated with an empirical coupled-channel approach. The P_{CN} is the probability that the system evolves from a touching configuration to the compound nucleus (CN) in competition with the quasifission. The last term W_{sur} is the survival probability of the formed compound nucleus, which can be estimated with a statistics model.

*baoxiaojun@hunnu.edu.cn

The capture cross section $\sigma_{\rm cap}(E_{\rm c.m.})$ at a given center-of-mass energy $E_{\rm c.m.}$ can be written as [36]

$$\sigma_{\rm cap}(E_{\rm c.m.}) = \frac{\pi\hbar^2}{2\mu E_{\rm c.m.}} \sum_J (2J+1) T(E_{\rm c.m.}, J), \tag{2}$$

where $E_{\rm c.m.}$ and J separately represent the incident energy in the center-of-mass system and the angular momentum. The $T(E_{\rm c.m.}, J)$ is the penetration probability of the two colliding nuclei overcoming the Coulomb potential barrier in the entrance channel. The capture cross section $\sigma_{\rm cap}(E_{\rm c.m.})$ can be estimated using the empirical coupled-channel method. According to the different coupling modes between the target and the projectile, we construct different barrier distribution functions. There are three cases: (i) fusion reactions involving two spherical nuclei, (ii) reactions with two statically deformed nuclei, and (iii) reactions with the combination of one spherical nucleus and one statically deformed nucleus, which are addressed in detail in Ref. [37].

The $P_{\rm CN}(E_{\rm c.m.}, J)$ in Eq. (1) is the probability of the evolution of the system from the contact configuration to the formation of the composite nucleus. The time evolution of the probability distribution function $P(Z_1, N_1, \beta_{12}, \beta_{22}, \theta_1, \theta_2, \varepsilon_1, t)$ at a fixed directional angle (θ_1 and θ_2) can be obtained by solving the master equation for the four variables in the corresponding potential energy surface [38], which is addressed in detail in Ref. [39].

Finally, the fusion probability is given by

$$\begin{aligned} P_{\rm CN}(E_{\rm c.m.}, J) = & \sum_{Z_1=1}^{Z_{\rm BG}} \sum_{N_1=1}^{N_{\rm BG}} \int_0^{\infty} \int_0^{\infty} \int_0^{\pi/2} \sin\theta_1 d\theta_1 \int_0^{\pi/2} \\ & \times P(Z_1, N_1, \beta_{12}, \beta_{22}, \theta_1, \theta_2, \tau_{\rm int}) \\ & \times \rho_1(\beta_{12}) \rho_2(\beta_{22}) d\beta_{12} d\beta_{22} \sin\theta_2 d\theta_2, \end{aligned} \tag{3}$$

where $N_{\rm BG}$ and $Z_{\rm BG}$ are the Businaro-Gallone (BG) points. The interaction time $\tau_{\rm int}$ in Eq. (3) determines how far the system travels along the potential energy surface, and the interaction time $\tau_{\rm int}$ in the dissipative process of two colliding nuclei is determined by using the deflection function method.

The survival probability $W_{\rm sur}(E_{\rm c.m.}, J)$ in Eq. (1) of the compound nucleus can be calculated using a statistical method. The survival probability of the excited compound nuclei during deexcitation by evaporation of neutrons competing with fission is expressed as follows:

$$W_{\rm sur}(E^*_{\rm CN}, x, J) = F(E^*_{\rm CN}, x, J) \prod_{i=1}^{x} \left[\frac{\Gamma_n(E^*_i, J)}{\Gamma_n(E^*_i, J) + \Gamma_f(E^*_i, J)} \right]_i, \tag{4}$$

where $F(E^*_{\rm CN}, x, J)$ is the realization probability [40] of the xn channel at the excitation energy $E^*_{\rm CN}(E_{\rm c.m.} + Q)$ of the compound nucleus with the angular momentum J, and i is the index of the evaporation step. The partial widths of neutron emission and fission are Γ_n [41,42] and Γ_f [43].

The level density is calculated using the back-shifted Fermi-gas model,

$$\rho(U, J) = \frac{(2J+1)\exp\left[2\sqrt{aU} - \frac{J(J+1)}{2\sigma^2}\right]}{24\sqrt{2}\sigma^3 a^{1/4} U^{5/4}}, \tag{5}$$

with $\sigma^2 = \frac{\Theta_{\rm rigid}}{\hbar^2}\sqrt{\frac{U}{a}}$, $\Theta_{\rm rigid} = \frac{2}{5} m_u A R^2$, and $U = E - \delta$. The back-shifts $\delta = -\Delta$(odd-odd), 0(odd-A), and Δ(even-even), respectively, are related to the neutron and proton pairing gap $\Delta = 1/2[\Delta_n(Z,N) + \Delta_p(Z,N)]$.

The dependence of the level-density parameter a on the shell correction and the excitation energy was proposed as

$$a(U, Z, N) = \tilde{a}(A)\left[1 + E_{\rm sh}\frac{f(U)}{U}\right], \tag{6}$$

with $\tilde{a}(A) = \alpha A + \beta A^{2/3}$ and $f(U) = 1 - \exp(-\gamma_D U)$. It should be noted that the differences between the corresponding level-density parameters are primarily due to different shell corrections. Thus, these parameters should be used at the same shell correction energies. The parameters $\alpha = 0.1337$, $\beta = -0.065\,71$, and $\gamma_D = 0.048\,84$ [44] determined by fitting to experimental level-density data with the help of the microscopic shell correction from FRDM95 [45] are adopted to calculate the level density used in the evaporation calculations.

III. NUMERICAL RESULTS AND DISCUSSIONS

To test the reliability of the DNS model, we now present the results of the theoretical calculation of the excitation functions for the ^{48}Ca-induced reactions with the target nuclei ^{238}U, ^{244}Pu, and ^{248}Cm and compare them with the available experimental data in Fig. 1, where the displayed error bars correspond to the statistical uncertainties only. For ^{48}Ca + ^{238}U [4,46], ^{48}Ca + ^{244}Pu [4,46–49], and ^{48}Ca + ^{248}Cm [4,46,50], taking into account the experimental uncertainties one can say that the agreement between our calculated ERCSs and the experimental data is good for most of the evaporation channels, especially in the 3n and 4n emission.

The above results give us the confidence to predict the ERCSs of fusion reactions leading to new superheavy nuclei, we calculate the evaporation residue cross section for the transition from ^{48}Ca to the fusion of the heavier projectiles (^{64}Ni, ^{58}Fe, ^{54}Cr, ^{50}Ti) with the target nuclei (^{238}U, ^{244}Pu, ^{248}Cm, ^{249}Cf), which is a possible alternative route to synthesize new superheavy nuclei. The present calculations for all reactions were performed with one set of parameters and with the same assumptions.

From Fig. 2(a), one can see that, when the ^{48}Ca projectile is replaced by ^{64}Ni, the ERCS 3n and 4n channels drop by 4 orders of magnitude. The maximal ERCSs of the 3n and 4n channels are 0.10 and 0.02 fb for the ^{64}Ni + ^{238}U reaction, respectively. The above ERCSs are 3 orders of magnitude below the present experimental technique limit (greater than 0.1 pb [5]). Note that efforts to synthesize the superheavy nucleus $Z = 120$ with the ^{64}Ni + ^{238}U reaction at GSI were unsuccessful [4,32].

The ERCSs for the 3n and 4n channels in the ^{58}Fe + ^{244}Pu reaction leading to the formation of ^{299}120 and ^{298}120 isotopes are evaluated, and the excitation functions of the ERCSs are shown in Fig. 2(b). The maximum ERCSs in the 3n and 4n evaporation channels are 4.11 and 0.36 fb, respectively. The above ERCSs are 2 orders of magnitude below the present experimental technique limit (greater than 0.1 pb [5]). In Dubna,

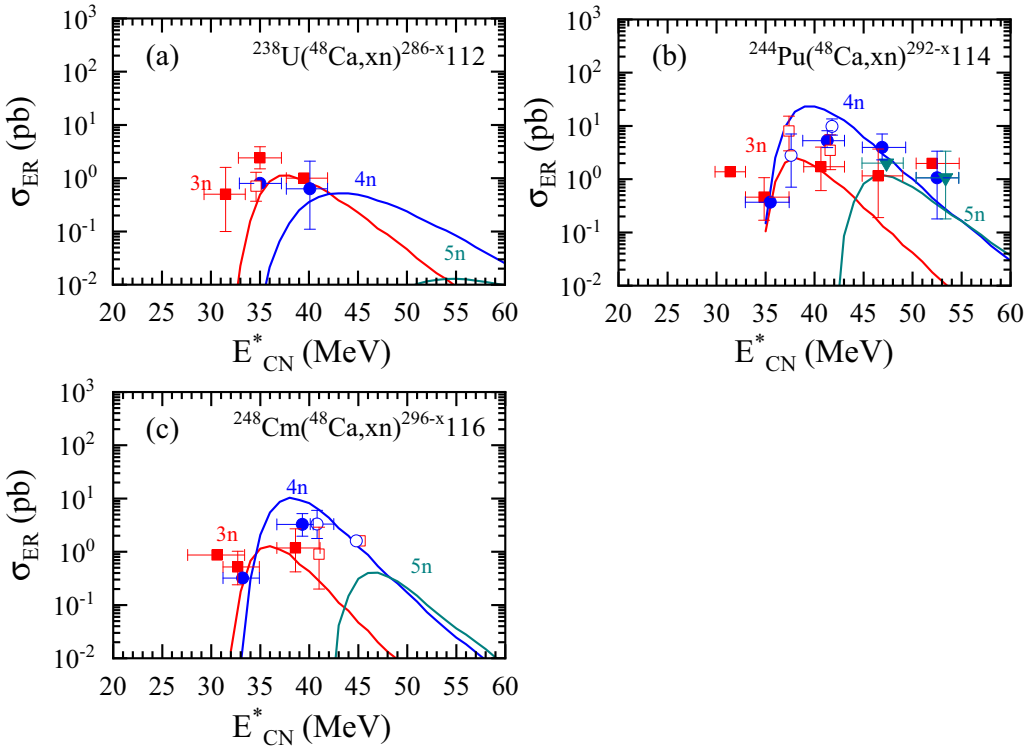

FIG. 1. The calculated ERCRs compared with the available experimental data for the reactions ^{48}Ca + ^{238}U [4,46], ^{48}Ca + ^{244}Pu [4,46–49], and ^{48}Ca + ^{248}Cm [4,46,50]. The measured ERCRs of the 3*n*, 4*n*, and 5*n* channels are denoted by red squares, blue circles, and dark cyan triangles, respectively. The corresponding theoretical values are represented by solid red lines, solid blue lines, and solid dark cyan lines. Experimental data from DGFRS (solid symbols) and SHIP, BGS, and TASCA (open symbols).

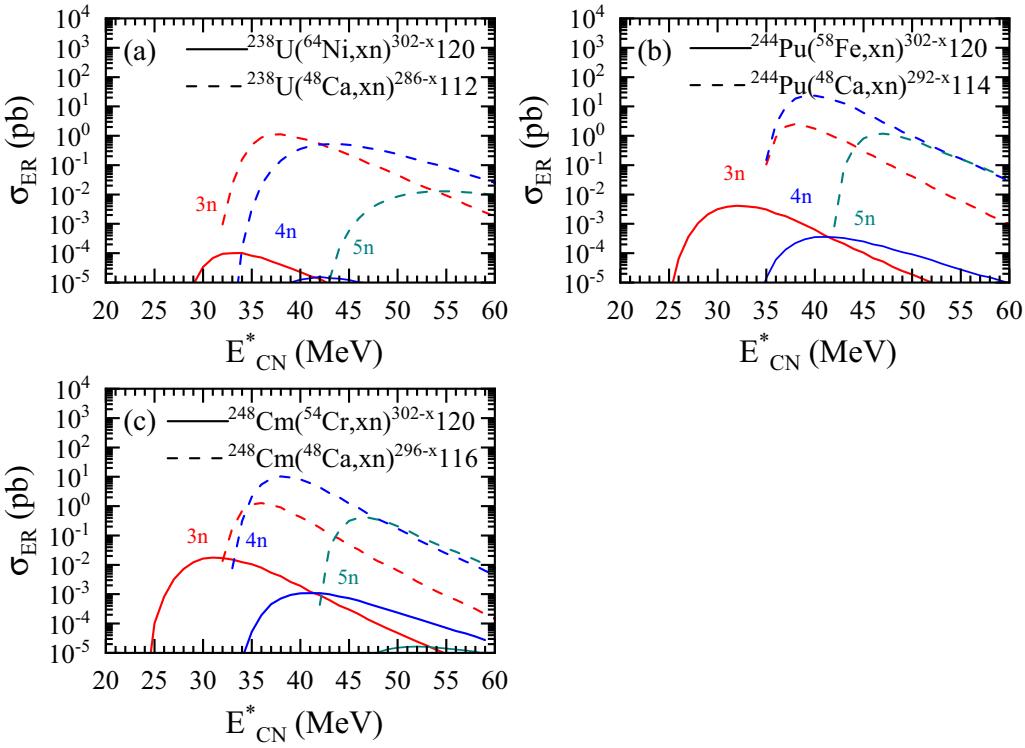

FIG. 2. The evaporation residue cross sections of ^{48}Ca + ^{238}U, ^{48}Ca + ^{244}Pu, and ^{48}Ca + ^{248}Cm (dashed lines) and of ^{64}Ni + ^{238}U, ^{58}Fe + ^{244}Pu, and ^{54}Cr + ^{248}Cm (solid lines) at 3*n*, 4*n*, and 5*n* channels are denoted by red, blue, and dark cyan lines, respectively.

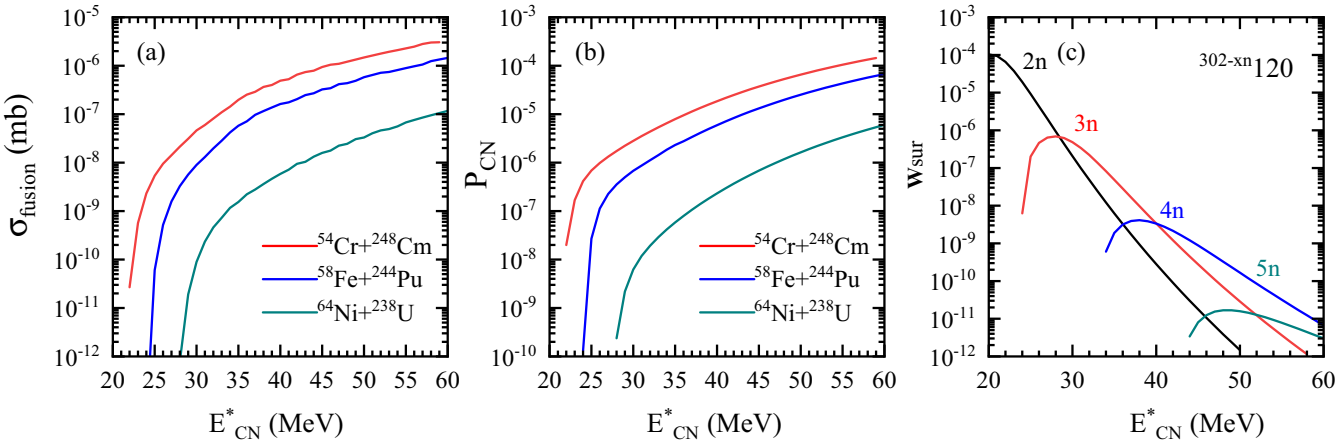

FIG. 3. The (a) calculated fusion cross sections and the (b) fusion probabilities as functions of excitation energy for the reactions $^{54}Cr + ^{248}Cm$, $^{58}Fe + ^{244}Pu$, and $^{64}Ni + ^{238}U$ are represented by red, blue, and dark cyan lines, respectively. The (c) survival probabilities are functions of the excitation energy of the compound nucleus. The $2n$, $3n$, $4n$, and $5n$ channels are represented by black, red, blue, and dark cyan lines, respectively.

attempts to synthesize superheavy nuclei with $Z = 120$ using the $^{58}Fe + ^{244}Pu$ reaction were unsuccessful [19].

Figure 2(c) shows the predicted excitation function of xn ERCSs for the reaction $^{54}Cr + ^{248}Cm$. The maximal ERCSs of the $3n$ and $4n$ channels are 17.58 and 1.09 fb, respectively. In Fig. 2(c), one can see that the ERCSs for ^{54}Cr and heavier projectiles with actinide targets are significantly lower compared to those of the ^{48}Ca-induced reaction of the same target reaction systems. The evaporation residual cross section in the $^{54}Cr + ^{248}Cm$ reaction system is approximately 3 orders of magnitude smaller than the measured result in the $^{48}Ca + ^{248}Cm$ reaction system. A new experimental study found [17] that the fusion probability of the $^{54}Cr + ^{248}Cm$ reaction decreases by a factor of 10^3 times compared to that of the $^{48}Ca + ^{248}Cm$ reaction. Among the reactions they studied, $^{54}Cr + ^{248}Cm$ was the most favorable for producing $Z = 120$ superheavy nuclei. Unfortunately, none of these experiments provided strong evidence for synthesizing new superheavy nuclei [17,18,22,24].

Similarly, in the heavy region, experimental results show strong influence of the entrance channel on the evaporation residue cross section. The xn excitation functions measured using the ^{50}Ti- and ^{54}Cr-induced reactions were compared those measured results for the ^{48}Ca-induced reactions with ^{162}Dy. Experimental results show that the evaporation residual cross section in the $^{54}Cr + ^{162}Dy$ reaction system is approximately 2 orders of magnitude smaller than the measured result in the $^{48}Ca + ^{162}Dy$ reaction system [51]. In the superheavy region, note that the evaporation residue cross section obtained from theoretical results for ^{54}Cr and heavier projectiles with actinide targets was significantly lower compared to that of the ^{48}Ca-induced reaction.

The estimation of fusion cross sections, fusion probability, and survival probability are shown in Fig. 3; these quantities have also been estimated by other authors and are useful for comparison. Based on the present results in Fig. 3, one can see that the main differences in the evaporative residue cross section of reactions $^{64}Ni + ^{238}U$, $^{58}Fe + ^{244}Pu$, and $^{54}Cr + ^{248}Cm$ leading to superheavy nuclei with $Z = 120$ could be strongly due to their entrance channel effects (capture cross section and fusion probability). One can argue that the $^{54}Cr + ^{248}Cm$ reaction with the smallest Z_pZ_t might be the most preferable for the making of the superheavy nuclei with $Z = 120$.

To illustrate the uncertainties in the predictions of the superheavy nuclei (SHN) production cross sections, we gather the anticipated findings from various models concerning the $^{54}Cr + ^{248}Cm$ reaction. Zagrebaev *et al.* [27] projected a nearly equivalent low cross section for the $^{54}Cr + ^{248}Cm$ reaction, with respective values of 15 and 28 fb. To calculate the survival probabilities, their work employed the fission barriers and other attributes of the SHN forecasted by the FRDM1995. Liu and Bao [26] using the modified fusion by diffusion model obtained 12 and 34 fb, respectively. According to the DNS model utilized by Nasirov *et al.* [28], nearly identical cross sections were obtained, with the maximum of ERCSs in the $3n$ and $4n$ channels being 16 and 14 fb, respectively. Their work adopted the the fission barrier heights [52] based on the Warsaw macroscopic-microscopic model [53] to calculate the survival probabilities. It can be observed that the ERCSs for the $^{54}Cr + ^{248}Cm$ reaction channel predicted by various theories are all in the range of a few femtobarns, which appears to be below the detectable limit of the currently available facilities.

Although all these theories give almost the same ERCS for the $^{54}Cr + ^{248}Cm$ reaction, a simple consistent result obtained from various theoretical results is not sufficient to reveal the essential substances of the phenomena involved. Actually, the fact is that all the above theories have provided approximately the same product $\sigma_{cap}P_{CN}W_{sur}$. We observed that each of the factors in Eq. (1) that affect the production of new heavy nuclei using complete fusions reactions has uncertainties.

Theoretically, the capture cross section in Eq. (1) is one of the important components in the synthesis of superheavy nuclei. The capture cross sections have been explored extensively, and most of them have tested a number of experimental data of capture cross sections; however, most do not lead

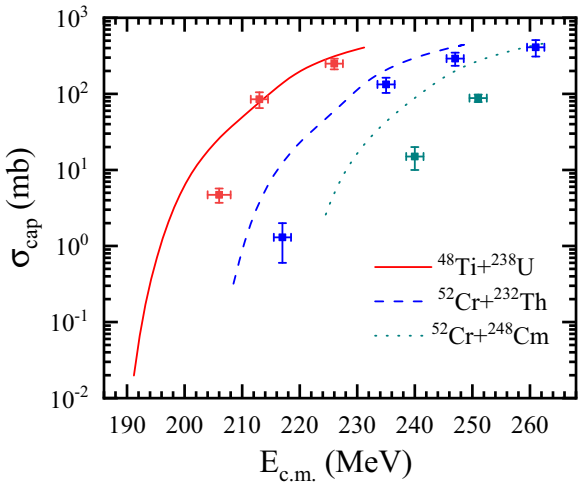

FIG. 4. The experimental values for $^{48}\mathrm{Ti} + ^{238}\mathrm{U}$, $^{52}\mathrm{Cr} + ^{232}\mathrm{Th}$, and $^{52}\mathrm{Cr} + ^{248}\mathrm{Cm}$ are represented by red squares, blue squares, and dark cyan squares, respectively [55]. The corresponding theoretical values are represented by the solid red line, the dashed blue line, and the dotted dark cyan line.

to the formation of the superheavy nuclei, especially for using projectiles $Z > 20$ to synthesize superheavy nuclei [54]. Therefore, it is very important to examine carefully the capture process for the study of the synthesis mechanism of superheavy nuclei.

Up to now, there have been no experimentally measured capture cross sections for the above mentioned three reaction systems. Very recently, the capture cross sections of the similar reaction systems $^{48}\mathrm{Ti} + ^{238}\mathrm{U}$, $^{52}\mathrm{Cr} + ^{232}\mathrm{Th}$, and $^{52}\mathrm{Cr} + ^{248}\mathrm{Cm}$ have been measured experimentally. As shown in Fig. 4, the theoretical calculations of $^{48}\mathrm{Ti} + ^{238}\mathrm{U}$, $^{52}\mathrm{Cr} + ^{232}\mathrm{Th}$, and $^{52}\mathrm{Cr} + ^{248}\mathrm{Cm}$ follow the trend of experimental measurements [55]. The ratio of calculated to observed capture cross sections varies from 1.35 to 3.50.

The fusion probability P_{CN} in Eq. (1) is one of the very important factors needed to calculate a ERCS; however, the fusion probability dependence on the excitation energy and the reaction entrance channel is still not well established. To calculate the fusion probability, the abovementioned various approaches and our models require the potential energy surface as input [26–28]. Various macroscopic-microscopic models have been widely used to estimate potential energy surface of the fusion process. However, the calculation of the multidimensional potential energy surface for the reaction system is a complicated physical problem, which has not yet been fully solved. This is because the proper choice of common degrees of freedom is an important and difficult task. The number of degrees of freedom should not be too large in order to allow the numerical analysis of the corresponding of dynamical equations. This means that the calculated potential energy surface is the upper limit of the optimum potential that the nucleus can adopt. Thus, the potential energy surface and the P_{CN} of heavy-ion fusion reactions are not fully understood.

The survival probability W_{sur} in Eq. (1) is affected by the fission barrier, the neutron separation energy, the level energy density parameter, the shell damping factor, and so on. The survival probability of compound nuclei, in particular, is highly sensitive to the fission barrier. Because our calculated ERCS is based on some nuclear data, such as nuclear mass, neutron separation energy, fission barrier (shell correction energy), and so on, the accuracy of our ERCS calculation is closely related to the accuracy of the extrapolation. In addition, these two different approaches to the damping of the shell effects will bring about quite different predictions of the survival probabilities [56,57]. In the present work, we adopt that the washing out of shell effects with increasing excitation energy is introduced in the nuclear level density parameter by proposing an exponential function.

Generally speaking, asymmetric systems are more favorable for the production of superheavy nuclei because the fusion probability strongly decreases with increasing the production of the charge numbers of projectile and target nuclei $Z_p Z_t$. However, since the absolute values of evaporation residue cross sections are dominated by the production of fusion and survival probabilities, in some cases the loss in the fusion probability for a more symmetric system may be compensated by the gain in the survival probability. Therefore, we also calculated the evaporative residue cross section for bombarding ^{50}Ti with ^{249}Cf.

In Fig. 5, our results of the $^{249}\mathrm{Cf}(^{50}\mathrm{Ti}, xn)^{299-xn}120$ and $^{248}\mathrm{Cm}(^{54}\mathrm{Cr}, xn)^{302-xn}120$ reactions are given. The maximum ERCSs in $3n$ and $4n$ evaporation channels are 2.14 and 0.16 fb for the $^{50}\mathrm{Ti} + ^{249}\mathrm{Cf}$ reaction, respectively. Recently, a search for the production of the superheavy elements with atomic numbers $Z = 120$ was performed at the gas-filled recoil separator TASCA at GSI using the $^{50}\mathrm{Ti} + ^{249}\mathrm{Cf}$ reaction. It was not detected at the cross-section sensitivity levels of 200 fb for the $^{50}\mathrm{Ti} + ^{249}\mathrm{Cf}$ reaction [2,15,16,22].

Displaying the predictions of other theoretical investigations could be quite interesting. By employing the DNS model for $^{50}\mathrm{Ti} + ^{249}\mathrm{Cf}$, Nasirov *et al.* [28] found that the ERCSs in the $3n$ and $4n$ channels are about 100 and 4 fb, respectively. Zagrebaev and Greiner [31] projected that the cross sections for the $3n$ and $4n$ channels in the $^{50}\mathrm{Ti} + ^{249}\mathrm{Cf}$ reaction would be approximately 40 fb. Siwek-Wilczýnska *et al.* [34] obtained the minimum ERCSs for the system $^{50}\mathrm{Ti} + ^{249}\mathrm{Cf}$ are about 6 fb in both the $3n$ and $4n$ channels, and for the $^{50}\mathrm{Ti} + ^{251}\mathrm{Cf}$ the minimum ERCS is about 0.70 fb for the $3n$ channel and 3 fb for the $4n$ channel. In the same reaction channels, Liu and Bao [58] predicted relatively higher cross sections; they predicted the ERCSs for the $3n$ and $4n$ channels from $^{50}\mathrm{Ti} + ^{249}\mathrm{Cf}$ to be approximately 90 and 50 fb, respectively. Sobiczewski *et al.* [34,59] indicate that the variation in these diverse theoretical results must primarily be attributed to the use of different fission barriers and ground-state masses in these calculations. Nevertheless, we would like to emphasize that those are only part of the reasons. In addition, these two different approaches to the damping of the shell effects will bring about quite different predictions of the survival probabilities [56,57]. It can be observed that the ERCSs for the $^{50}\mathrm{Ti} + ^{249}\mathrm{Cf}$ reaction channel predicted by various theories are all in the range of a few femtobarns, which appears to be below the detectable limit of the currently available facilities.

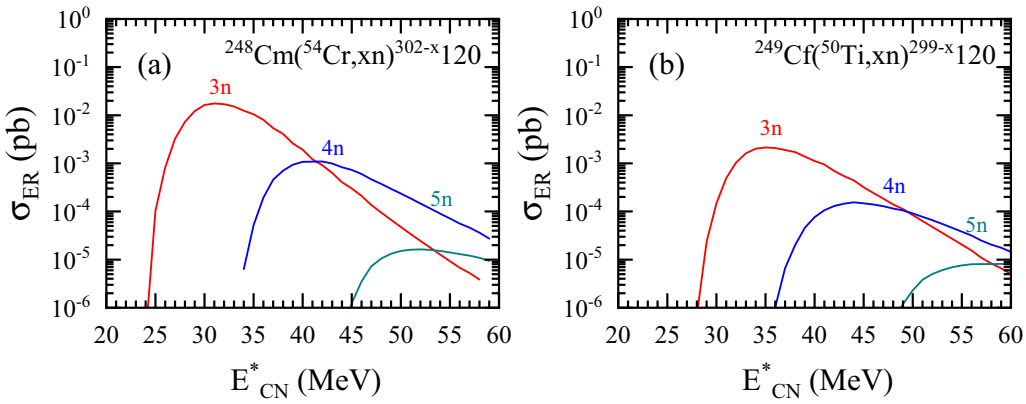

FIG. 5. Evaporation residue cross sections of ^{54}Cr + ^{248}Cm and ^{50}Ti + ^{249}Cf with 3*n*, 4*n*, and 5*n* channels are indicated by solid red lines, solid blue lines, and solid dark cyan lines, respectively.

IV. SUMMARY

In the present work, the capture cross section $\sigma_{\rm cap}(E_{\rm c.m.})$ can be estimated using the empirical coupled-channel method. According to the different coupling modes between the target and the projectile, we construct different barrier distribution functions. For the fusion probability, within the DNS concept, by taking the deformations of interacting nuclei as independent dynamical variables, the evolution of the DNS toward quasifission and fusion is treated as a diffusion process by solving four-variable master equations. In this way, the driving potential for nucleon transfer follows the time-dependent nuclear deformation to become time dependent; therefore, actually the evolutions of the four dynamical variables (N_1, Z_1, β_1, β_2) as well as their correlations are treated at the same time. For the survival probability, we adopt that the washing out of shell effects with increasing excitation energy is introduced in the nuclear level density parameter by proposing an exponential function. Finally, the evaporation residual cross sections in ^{48}Ca-induced hot-fusion reactions that produce SHN are systematically investigated. The calculated results reproduce well the experimental trends of the 3*n*- and 4*n*-channel cross sections of ^{48}Ca + ^{238}U, ^{48}Ca + ^{244}Pu, and ^{48}Ca + ^{248}Cm.

For the synthetic new element $Z = 120$, we predicted evaporation residue cross sections for four reaction systems (^{54}Cr + ^{248}Cm, ^{58}Fe + ^{244}Pu, ^{64}Ni + ^{238}U, and ^{50}Ti + ^{249}Cf) to select the most promising projectile-target combinations. By detailed analysis of the evaporation residue cross sections of synthetic superheavy nuclei, we found that the ^{54}Cr + ^{248}Cm reaction is optimal and the maximum cross sections of 3*n* and 4*n* channels are 17.58 and 1.09 fb. However, we also noticed that the ERCSs for the ^{54}Cr + ^{248}Cm reaction channel predicted by our model and various other approaches are all in the range of a few femtobarns, which appears to be below the detectable limit of the currently available facilities. Thus, an increase of beam intensities, detection techniques, and efficient separation are needed to synthesize $Z = 120$ superheavy nuclei. We hope that some results and discussions in this paper can provide some help for the experimental synthesis of new elements.

ACKNOWLEDGMENTS

The National Natural Science Foundation of China (Grants No.12175064 and No. U2167203) and the Hunan Outstanding Youth Science Foundation (Grant No. 2022JJ10031).

[1] B. B. Back, H. Esbensen, C. L. Jiang, and K. E. Rehm, Rev. Mod. Phys. **86**, 317 (2014).
[2] A. Di Nitto *et al.*, Phys. Lett. B **784**, 199 (2018).
[3] Yu. T. Oganessian and V. K. Utyonkov, Nucl. Phys. A **944**, 62 (2015).
[4] Yu. T. Oganessian *et al.*, Phys. Rev. C **74**, 044602 (2006).
[5] S. Hofmann, J. Phys. G: Nucl. Part. Phys. **42**, 114001 (2015).
[6] S. Hofmann and G. Münzenberg, Rev. Mod. Phys. **72**, 733 (2000).
[7] S. Hofmann *et al.*, Eur. Phys. J. A **14**, 147 (2002).
[8] K. Morita *et al.*, J. Phys. Soc. Jpn. **76**, 043201 (2007).
[9] Yu. T. Oganessian *et al.*, Phys. Rev. C **83**, 054315 (2011).
[10] Yu. T. Oganessian *et al.*, Phys. Rev. C **87**, 014302 (2013).
[11] Yu. T. Oganessian and V. K. Utyonkov, Rep. Prog. Phys. **78**, 036301 (2015).
[12] V. K. Utyonkov *et al.*, Phys. Rev. C **92**, 034609 (2015).
[13] E. M. Holmbeck, T. M. Sprouse, and M. R. Mumpower, Eur. Phys. J. A **59**, 28 (2023).
[14] B. Lommel, C. E. Düllmann, B. Kindler, and D. Renisch, Eur. Phys. J. A **59**, 14 (2023).
[15] J. Khuyagbaatar *et al.*, Phys. Rev. C **102**, 064602 (2020).
[16] K. Jadambaa, EPJ Web Conf. **163**, 00030 (2017).
[17] K. V. Novikov *et al.*, Phys. Rev. C **102**, 044605 (2020).
[18] S. Hofmann *et al.*, Eur. Phys. J. A **52**, 180 (2016).
[19] Yu. T. Oganessian *et al.*, Phys. Rev. C **79**, 024603 (2009).
[20] E. M. Kozulin *et al.*, Phys. Lett. B **686**, 227 (2010).
[21] G. N. Knyazheva, A. A. Bogachev, I. M. Itkis, M. G. Itkis, and E. M. Kozulin, AIP Conf. Proc. **1224**, 377 (2010).
[22] H. M. Albers *et al.*, Phys. Lett. B **808**, 135626 (2020).
[23] K. V. Novikov *et al.*, Bull. Russ. Acad. Sci. Phys. **84**, 495 (2020).

[24] F. P. Heßberger and D. Ackermann, Eur. Phys. J. A **53**, 123 (2017).
[25] G. Mandaglio, A. K. Nasirov, F. Curciarello, V. D. Leo, M. Romaniuk, G. Fazio, and G. Giardina, J. Phys.: Conf. Ser. **420**, 012008 (2013).
[26] Z.-H. Liu and J.-D. Bao, Phys. Rev. C **87**, 034616 (2013).
[27] V. Zagrebaev, A. Karpov, and W. Greiner, Acta Phys. Pol., B **45**, 291 (2014).
[28] A. K. Nasirov, G. Mandaglio, G. Giardina, A. Sobiczewski, and A. I. Muminov, Phys. Rev. C **84**, 044612 (2011).
[29] K. Siwek-wilczyńska, T. Cap, and J. Wilczyński, Int. J. Mod. Phys. E **19**, 500 (2010).
[30] Y.-J. Liang, M. Zhu, Z.-H. Liu, and W.-Z. Wang, Phys. Rev. C **86**, 037602 (2012).
[31] V. Zagrebaev and W. Greiner, Phys. Rev. C **78**, 034610 (2008).
[32] C. E. Düllmann, EPJ Web Conf. **163**, 00015 (2017).
[33] Z.-Q. Feng, G.-M. Jin, J.-Q. Li, and W. Scheid, Nucl. Phys. A **816**, 33 (2009).
[34] K. Siwek-Wilczyńska, T. Cap, M. Kowal, A. Sobiczewski, and J. Wilczyński, Phys. Rev. C **86**, 014611 (2012).
[35] C. C. Sahm, H. G. Clerc, K.-H. Schmidt, W. Reisdorf, P. Armbruster, F. P. Hessberger, J. G. Keller, G. Münzenberg, and D. Vermeulen, Nucl. Phys. A **441**, 316 (1985).
[36] C. Y. Wong, Phys. Rev. Lett. **31**, 766 (1973).
[37] G. J. Li and X. J. Bao, Phys. Rev. C **107**, 024611 (2023).
[38] X. J. Bao, S. Q. Guo, J. Q. Li, and H. F. Zhang, Phys. Lett. B **785**, 221 (2018).
[39] X. J. Bao, Nucl. Phys. A **986**, 60 (2019).
[40] J. D. Jackson, Can. J. Phys. **34**, 767 (1956).
[41] I. Dostrovsky, Z. Fraenkel, and G. Friedlander, Phys. Rev. **116**, 683 (1959).
[42] X. J. Bao, Chin. Phys. C **43**, 054105 (2019).
[43] N. Bohr and J. A. Wheeler, Phys. Rev. **56**, 426 (1939).
[44] T. Rauscher, F.-K. Thielemann, and K.-L. Kratz, Phys. Rev. C **56**, 1613 (1997).
[45] P. Moller, J. R. Nix, W. D. Myers, and W. J. Swiatecki, At. Data Nucl. Data Tables **59**, 185 (1995).
[46] Yu. T. Oganessian *et al.*, Phys. Rev. C **70**, 064609 (2004).
[47] J. M. Gates *et al.*, Phys. Rev. C **83**, 054618 (2011).
[48] Yu. T. Oganessian *et al.*, Phys. Rev. C **69**, 054607 (2004).
[49] C. E. Düllmann *et al.*, Phys. Rev. Lett. **104**, 252701 (2010).
[50] S. Hofmann *et al.*, Eur. Phys. J. A **48**, 62 (2012).
[51] D. A. Mayorov, T. A. Werke, M. C. Alfonso, E. E. Tereshatov, M. E. Bennett, M. M. Frey, and C. M. Folden, Phys. Rev. C **92**, 054601 (2015).
[52] M. Kowal, P. Jachimowicz, and A. Sobiczewski, Phys. Rev. C **82**, 014303 (2010).
[53] I. Muntian, Z. Patyk, and A. Sobiczewski, Phys. At. Nucl. **66**, 1015 (2003).
[54] B. Wang, K. Wen, W.-J. Zhao, E.-G. Zhao, and S.-G. Zhou, At. Data Nucl. Data Tables **114**, 281 (2017).
[55] M. G. Itkis, G. N. Knyazheva, I. M. Itkis, and E. M. Kozulin, Eur. Phys. J. A **58**, 178 (2022).
[56] N.-N. Li and X.-J. Bao, Chin. Phys. C **44**, 094102 (2020).
[57] W. Reisdorf, Z. Phys. A **300**, 227 (1981).
[58] Z. H. Liu and J.-D. Bao, Phys. Rev. C **80**, 054608 (2009).
[59] G. Mandaglio, G. Giardina, A. K. Nasirov, and A. Sobiczewski, Phys. Rev. C **86**, 064607 (2012).